

## Submonolayer phases of Pb on Si(111)

Eric Ganz, Fulin Xiong, Ing-Shouh Hwang, and Jene Golovchenko

*Department of Physics and Division of Applied Sciences, Harvard University, Cambridge, Massachusetts 02138*

(Received 16 October 1990)

We present conclusive results on the structures and coverages of the submonolayer phases of Pb on the Si(111)  $7\times 7$  surface based on scanning-tunneling-microscopy, low-energy-electron-diffraction, and Rutherford backscattering measurements. For room-temperature deposition at low coverage on the  $7\times 7$  surface, we find that Pb atoms occupy sites above and between the Si adatoms (with a preference for the faulted half of the unit cell) leaving the  $7\times 7$  structure intact. After annealing to 450°C, some Pb atoms occupy Si(111)  $7\times 7$  adatom sites, while others have nucleated to form small areas of an unusual  $\sqrt{3}\times\sqrt{3}$  phase which has a 1:1 ratio of Si:Pb.

In recent years there has been significant interest in thin metal films on semiconductors. From a technological standpoint, these films are important in the fabrication of integrated circuits. There has also been an effort to understand the formation of Schottky barriers on an atomic scale. In particular, Pb/Si(111) has been proposed as a model system because Pb and Si have negligible mutual bulk solubility.<sup>1,2</sup> Thus, the Pb/Si system is remarkably unreactive, and ought to provide a relatively simple interface to study. Recently, Heslinga *et al.*<sup>3</sup> reported that the Schottky barrier height for Pb/Si(111) contacts depended strongly on the interface structure which they modified by annealing. Furthermore, both Pb/Si(111) and Pb/Ge(111) have been proposed as candidates for studies of two-dimensional (2D) melting.<sup>4</sup> Unfortunately, there has been considerable confusion and controversy regarding the atomic structure, coverage, and even the number of distinct phases of Pb/Si(111).<sup>1,5-8</sup> This is, in part, due to the fact that Pb/Si(111) has a complex phase diagram in which coverage, temperature, and annealing history are all important. The lack of accurate coverage measurements and the use of indirect probes have allowed this confusion to persist for many years. In this paper we provide an accurate and conclusive understanding of the low-coverage regime of Pb/Si(111) based upon Rutherford backscattering spectroscopy (RBS), thermal desorption measurements, low-energy electron diffraction (LEED), and scanning tunneling microscopy (STM). We will show that despite the negligible mutual solubility in the bulk, conditions at the surface can conspire to mix the Pb and Si adatoms.

Pb/Si(111) was first studied by Estrup and Morrison<sup>9</sup> in 1964 using LEED. For room-temperature (RT) deposition, they proposed epitaxial growth of Pb on Si(111)  $7\times 7$ . After annealing, the  $7\times 7$  periodicity was destroyed, and two  $\sqrt{3}\times\sqrt{3}$  patterns were observed. They proposed models with coverages of  $\frac{1}{3}$  and  $\frac{4}{3}$  ML (monolayer), respectively ( $1\text{ ML}=7.84\times 10^{14}$  Pb atoms/cm<sup>2</sup>). These results were confirmed and extended by Saitoh *et al.*<sup>5</sup> using low-energy ion scattering and LEED in 1983. Subsequently, LeLay and co-workers<sup>1,6,7</sup> have applied LEED, Auger, ellipsometry, thermal desorption,

and ultraviolet photoemission spectroscopy to study this system. They reported three different  $\sqrt{3}\times\sqrt{3}$  phases at  $\frac{1}{3}$ ,  $\frac{2}{3}$ , and 1 ML, respectively. Recently, Grey *et al.*<sup>8</sup> have used x-ray diffraction to study the 1-ML phases: with no annealing, they proposed a modified  $8\times 8$  Pb layer on the  $7\times 7$  Si substrate, while for an annealed surface they found a 30° rotated incommensurate layer.

Our experiments were performed in two UHV chambers. Each chamber contains a Pb effusion cell, sample exchange, sample heating capability, ion sputtering, and a rear view LEED apparatus. The STM chamber has a base pressure of  $6\times 10^{-11}$  Torr. The RBS measurements were done in a UHV beamline with a base pressure of  $1.5\times 10^{-10}$  Torr connected to a General Ionex 1.7 MeV Tandem Accelerator. A 2-MeV He<sup>+</sup> beam was delivered to the chamber through a 2-mm aperture in a differentially pumped beam line. Scattered ions were detected by a Si solid-state detector [20-keV full width at half-maximum (FWHM) resolution] which was set at a scattering angle of 170° with respect to the incident beam. 99.999% purity Pb was evaporated from an effusion cell at 480°C at a rate of 1 ML/min from a distance of 10 cm. We used 1  $\Omega$  cm *p*-type Si(111) wafers which were Shiraki etched,<sup>10</sup> mounted using Ta clips, and degassed by resistive heating in UHV at 600°C overnight. The samples were then annealed to 920°C for several minutes and cooled at 1°C/sec. This process consistently produced very sharp  $7\times 7$  LEED patterns. Sample temperature was measured with an optical pyrometer. The pressure was maintained at less than  $5\times 10^{-10}$  Torr during both sample preparation and Pb deposition, and no impurities in the Pb films were detectable using RBS or x-ray photoemission spectroscopy (XPS). Samples could be cleaned for reuse either by heating to 850°C, or by ion sputtering and annealing. STM images of the clean Si(111)  $7\times 7$  showed large terraces (500 Å) of nearly perfect  $7\times 7$  structure. Some samples were transferred in air from the STM chamber to the accelerator for coverage measurements, and to calibrate the STM effusion cell. The STM was run at 100-pA constant tunneling current, with +2-V bias on the sample. In the images, the gray scale reflects the sample height and electronic structure,

with white above black by roughly  $3 \text{ \AA}$ .

We will begin by discussing the STM results for the low coverage RT deposited cases. In Fig. 1(a) we show the result of depositing a very small amount (0.05 ML) of Pb onto the clean Si(111)  $7 \times 7$  surface at RT. The Pb forms triangles of three Pb atoms preferentially covering the faulted side of the  $7 \times 7$  unit cell. The faulted and unfaulted halves of the Si(111)  $7 \times 7$  unit cell were distinguished by tunneling with  $-1.7\text{-V}$  bias on the sample

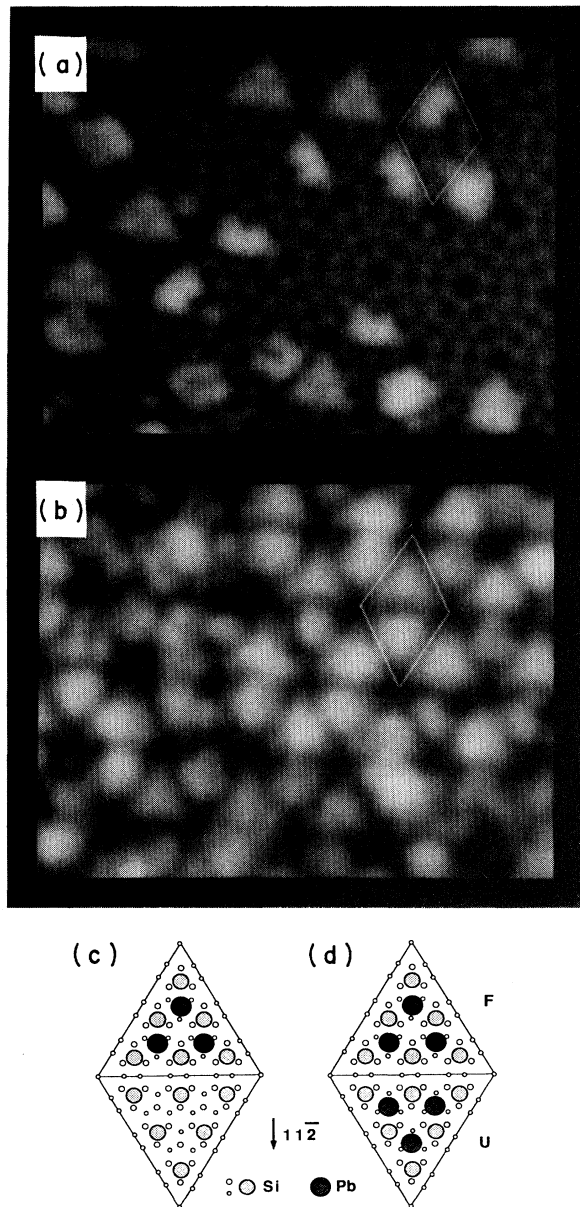


FIG. 1.  $120 \times 140 \text{ \AA}^2$  tunneling images of (a) 0.04-ML Pb, and (b) 0.15-ML Pb deposited onto Si(111)  $7 \times 7$  at RT. Models showing Pb adatom positions for (c) 0.06-ML Pb, and (d) 0.12-ML Pb. The Pb adatoms are above and between the Si adatoms. Small circles represent first and second Si substrate layer, large circles represent Si and Pb adatoms. The faulted and unfaulted halves of the  $7 \times 7$  unit cell are indicated.

(not shown).<sup>11</sup> The Pb atoms in these triangles generally sit at sites above and between the Si adatoms, and the underlying Si(111)  $7 \times 7$  reconstruction is relatively unchanged. We measured  $2 \pm 0.5 \text{ \AA}$  vertical distance from the top of the Si adatoms to the top of the Pb adatoms. This value may be too large due to the effect of electronic structure on the STM image. Figure 1(c) is a model for this phase based upon the dimer-adatom-stacking fault (DAS) model of Takanayagi *et al.*<sup>12</sup> Figure 1(a) also shows single Pb atoms and pairs of atoms on this site. Finally, there is occasionally a Pb atom in the Si adatom site (a  $T_4$  site on the Si substrate): this atom may have filled a Si adatom vacancy that existed before the evaporation. The preferential occupation of the faulted half of the unit cell has been observed in Ag/Si and Pd/Si experiments.<sup>13,14</sup> However, both of those systems are significantly more reactive than Pb/Si, and involve intermixing of Pd or Ag with Si. Therefore, it is more difficult to determine the origin of the preferential occupation for the Ag and Pd experiments. We suggest that the Pb selects the faulted side because the density of filled states is slightly higher than on the unfaulted side.

In Fig. 1(b) we show the result of depositing 0.15-ML Pb onto the clean Si(111)  $7 \times 7$  surface at RT. We see that the entire  $7 \times 7$  unit cell is now covered with Pb atoms. We still observe sets of three Pb atoms forming triangular features. In Fig. 1(d) we show a model for this coverage. We observe excess Pb atoms randomly distributed across the surface, and in the centers of the triangles. The LEED patterns for the samples studied in Fig. 1 showed  $7 \times 7$  periodicity, but with reduced intensity and increased background. This is consistent with our model: at low coverage (less than 0.12 ML), the Pb atoms are aligned with the  $7 \times 7$  substrate (albeit with a  $2 \times 2$  spacing), while at higher coverage (0.12–0.5 ML), we observe increasing disorder in the Pb layer, but with the  $7 \times 7$  periodicity still evident. Thus, before annealing, the Pb and Si do not intermix.

When the Pb/Si samples are annealed to  $450^\circ\text{C}$ , the Pb/Si interface can equilibrate to form new structures. We present LEED results obtained along with isothermal desorption of 1-ML Pb deposited at RT on Si(111)  $7 \times 7$  which allows us to separate and identify the annealed submonolayer phases. Two isothermal desorption spectra are shown in Fig. 2. The Pb coverage measurements were made at RT using RBS. The annealing was done at two different temperatures with extension of annealing time in intervals of 1–3 min. In Fig. 2, four distinct phases between 0 and 1 ML are distinguished. Above 0.8 ML (A) the LEED pattern shows the rotated incommensurate phase. At 1 ML this phase transforms above roughly  $200^\circ\text{C}$  to a  $1 \times 1$  LEED pattern. The incommensuration and melting point of this phase vary with coverage. At 0.8 ML (B) we observe a  $1 \times 1$  LEED pattern stable at RT. At  $\frac{1}{3}$  ML (C) a  $\sqrt{3} \times \sqrt{3}$  pattern is obtained. At  $\frac{1}{6}$  ML (D) the LEED pattern is similar to the  $\sqrt{3} \times \sqrt{3}$  at  $\frac{1}{3}$  ML, but the spots are brighter. At intermediate coverages, the surface contains mixed phases. We observe neither the spot extinctions at 40 eV nor the  $\frac{2}{3}$ -ML phase reported by LeLay, Peretti, and Hanbucken.<sup>1</sup> When the  $7 \times 7$  reconstruction of the Si surface is

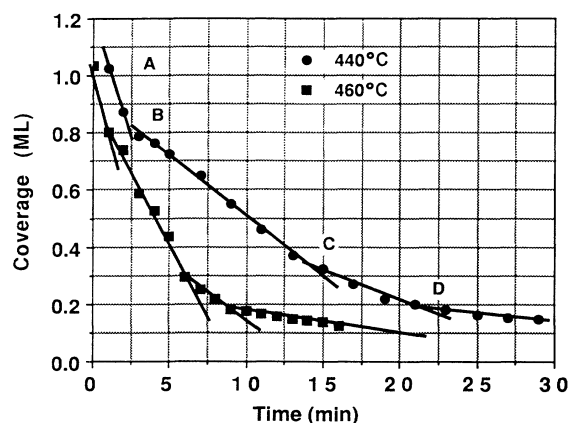


FIG. 2. Isothermal desorption curves of 1 ML of Pb/Si(111) at 440°C and 460°C. Four different phases are visible: above 0.8 ML (A) incommensurate phase, at 0.8 ML (B)  $1 \times 1$  phase, at  $\frac{1}{3}$  ML (C)  $\sqrt{3} \times \sqrt{3}$  phase, at  $\frac{1}{6}$  ML (D) mixed Si:Pb  $\sqrt{3} \times \sqrt{3}$  phase.

destroyed, 7 of the 12 adatoms are used to fill the corner hole and stacking fault, leaving 5 adatoms per unit cell or 0.1 ML Si. If these Si adatoms do not have time to migrate to step edges or nucleate islands, they may mix with the Pb overlayer. This accounts for the fact that the condition B in Fig. 2 occurs slightly below 1 ML. The curves in Fig. 2 were generated from a sample with Pb evaporated onto clean Si(111)  $7 \times 7$ . If, instead, the sample is prepared by evaporating 1-ML Pb onto the  $\frac{1}{6}$ -ML phase, then the desorption curve does not show a separate phase at  $\frac{1}{3}$  ML. This may explain the thermal desorption curves published by Saitoh *et al.*<sup>5</sup> which actually show a new phase at  $\frac{1}{6}$  ML instead of  $\frac{1}{3}$  ML as claimed. Isothermal desorption spectra for lower annealing temperatures and higher coverages will be discussed in a subsequent paper.

We have studied this new  $\frac{1}{6}$ -ML  $\sqrt{3} \times \sqrt{3}$  phase using the STM. In Fig. 3 we show two tunneling images of a sample with mixed  $\sqrt{3} \times \sqrt{3}$  and  $7 \times 7$  phases. This sample was prepared by evaporating 0.06-ML Pb onto Si(111)  $7 \times 7$  at RT, and then annealing to 450°C. Most of the sample remained  $7 \times 7$ , with small isolated areas of  $\sqrt{3} \times \sqrt{3}$ . The LEED pattern showed both sharp  $\sqrt{3} \times \sqrt{3}$  and  $7 \times 7$  spots. Figure 3(a) shows an STM image with a  $7 \times 7$  area on the left and a  $\sqrt{3} \times \sqrt{3}$  area on the right. The boundary between the phases is relatively sharp, with some missing Si adatoms. By triangulating from the  $7 \times 7$  structure, we find that the atoms in the  $\sqrt{3} \times \sqrt{3}$  phase sit at  $T_4$  sites [on the Si(111) surface]. The image in Fig. 3(a) was obtained with a +1.65-V bias on the sample. At this bias, the Pb and Si atoms are indistinguishable. If we raise the bias to +2.3 V, the Pb atoms appear higher (brighter) because the tunneling current is enhanced at these sites. Figure 3(b) shows the same location as Fig. 3(a), but now the Pb atoms are visible as white spots. We note that the Pb atoms in the  $\sqrt{3} \times \sqrt{3}$  area are not randomly distributed, but appear to form chains. This behavior is analogous to that of a

two-dimensional hexagonal antiferromagnetic Ising model: the system can minimize the number of same species nearest neighbors by forming chains. From the isothermal desorption curves shown in Fig. 2 we conclude that the ideal density for the mixed Si:Pb  $\sqrt{3} \times \sqrt{3}$  phase is  $\frac{1}{6}$  ML (1:1 Pb:Si ratio). We have also imaged annealed samples with higher Pb coverage: at  $\frac{1}{3}$  ML the sample is

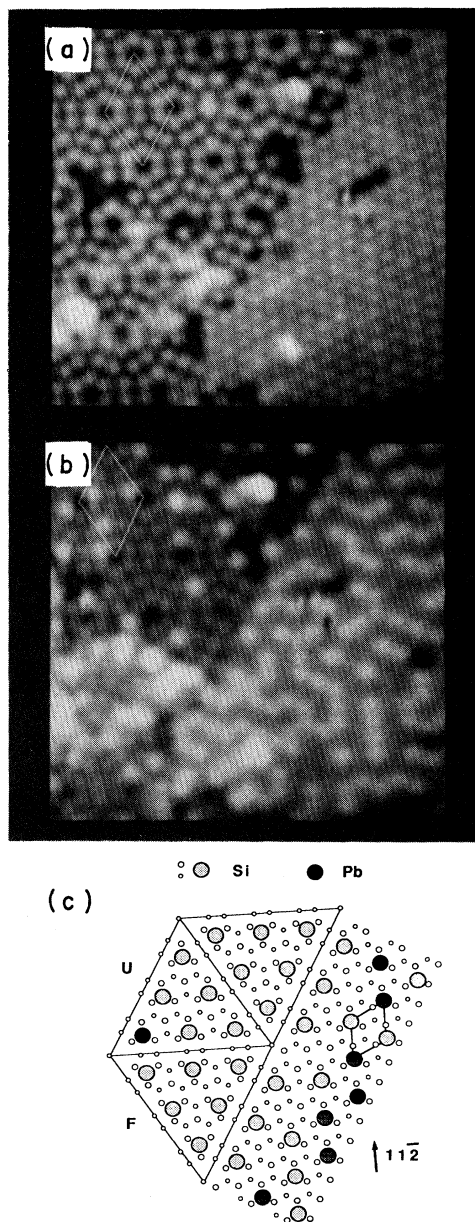


FIG. 3. Two  $150 \times 150 \text{ \AA}^2$  tunneling images of an interface between  $7 \times 7$  and  $\sqrt{3} \times \sqrt{3}$  areas. (a) At 1.65-V bias, Pb and Si atoms are indistinguishable. (b) At 2.3-V bias the Pb atoms appear as bright spots. (c) Model showing the atomic arrangement of the interface at the center of (a) and (b). Small circles represent first and second Si substrate layer, large circles represent Si and Pb adatoms. The faulted and unfaulted halves of the  $7 \times 7$  unit cell are indicated.

covered with  $\sqrt{3}\times\sqrt{3}$  structure formed almost entirely of Pb. Figure 3(c) shows a model of the interface between this  $\sqrt{3}\times\sqrt{3}$  phase and the  $7\times 7$  phase, corresponding to the center of Figs. 3(a) and 3(b). The boundary is parallel to, but offset from, the dimer chains of the Si(111)  $7\times 7$  which may indicate that it is favorable for Si adatoms to occupy sites next to the dimer chains.

In Fig. 3(b), we see that Pb atoms can replace the Si adatom site in the  $7\times 7$  lattice at very low density in these annealed samples. Furthermore, the density of Pb in the  $\sqrt{3}\times\sqrt{3}$  areas (0.14 ML) is much higher than the density of Pb in the  $7\times 7$  areas (0.04 ML). If we recall that we deposited 0.06-ML Pb, we conclude that the Pb atoms are mobile during the anneal, and concentrate at the growing  $\sqrt{3}\times\sqrt{3}$  islands. This mobility suggests that the Pb forms a 2D gas phase at elevated temperatures. LeLay, Manneville, and Kern<sup>15</sup> have proposed a 2D gas phase model to explain the observation of zero-order thermal desorption kinetics for Au/Si(111). This model has also been proposed for the desorption of Pb/Ge(111).<sup>16</sup> We note that our thermal desorption results (Fig. 2) are consistent with zero-order kinetics for this phase. If the Pb forms a 2D gas at elevated temperatures, then the density of Pb atoms in the  $7\times 7$  areas will be determined by the annealing temperature.

In this paper we have discussed the atomic structure of Pb/Si(111) interfaces at low coverages. By combining the accurate coverage measurements of the RBS with the

overview of the LEED and the local atomic view of the STM, we have obtained a detailed understanding of a complex and inhomogeneous system. For low coverages at room temperature, STM images show that the Pb atoms occupy sites above and between the Si(111)  $7\times 7$  adatoms. During isothermal desorption, we observe phase transitions at 0.8, 0.33, and 0.16 ML. Finally, the STM has revealed a new  $\frac{1}{6}$ -ML  $\sqrt{3}\times\sqrt{3}$  phase which shows a mixture of Pb and Si adatoms at  $T_4$  sites. The existence of mixed phases and mixed atomic occupation of phases conspire to make this system difficult to study using nonlocal techniques like LEED or x-ray diffraction. Extensions of this work should lead to a better understanding of Schottky barrier formation as the STM provides the possibility of measurements of the local electronic structure of surfaces.<sup>17</sup> We plan to report on the higher coverage cases and address issues of domain size and melting in a subsequent paper.

We would like to thank Silva Leonard, Dongmin Chen, David Vanderbilt, Bill Foster, and Anthony Loeser for helpful discussions and assistance. This research was supported by the Office of Naval Research (Contract No. N00014-90-J-1234), the Materials Research Laboratory at Harvard University (Contract No. NSF-DMR-8920490), and the Joint Services Electronics Program (Contract No. N00014-89-J-1023).

- 
- <sup>1</sup>G. LeLay, J. Peretti, and M. Hanbucken, *Surf. Sci.* **204**, 57 (1988).  
<sup>2</sup>R. W. Olesinski and G. J. Abbaschian, *Bull. Alloy Phase Diagrams* **5**, 271 (1984).  
<sup>3</sup>D. R. Heslinga, H. H. Weitering, D. P. van der Werf, T. M. Klapwijk, and T. Hibma, *Phys. Rev. Lett.* **64**, 1589 (1990).  
<sup>4</sup>T. Ichikawa, *Solid State Commun.* **46**, 827 (1983); **49**, 59 (1984).  
<sup>5</sup>M. Saitoh, K. Oura, K. Asano, F. Shoji, and T. Hanawa, *Surf. Sci.* **154**, 394 (1985).  
<sup>6</sup>G. Quentel, M. Gauch, and A. Degiovanni, *Surf. Sci.* **193**, 212 (1988).  
<sup>7</sup>G. LeLay, K. Hricovini, and J. E. Bonnet, *Appl. Surf. Sci.* **41/42**, 25 (1989).  
<sup>8</sup>F. Grey, R. Feidenhans'l, M. Nielsen, and R. L. Johnson, *Colloq. Phys.* **C7**, 181 (1989); R. Feidenhans'l, F. Grey, M. Nielsen, and R. L. Johnson, in *Kinetic of Ordering and Growth at Surfaces*, edited by M. Lagally (NATO Advanced Research Workshop) (in press).  
<sup>9</sup>P. J. Estrup and J. Morrison, *Surf. Sci.* **2**, 465 (1964).  
<sup>10</sup>A. Ishizaka, N. Nakagawa, and Y. Shiraki, in *Proceedings of the 2nd International Symposium on Molecular Beam Epitaxy* (Japanese Society of Applied Physics, Tokyo, 1982), p. 182.  
<sup>11</sup>R. M. Tromp, R. J. Hamers, and J. E. Demuth, *Phys. Rev. B* **15**, 1388 (1986).  
<sup>12</sup>K. Takayanagi, Y. Tanishiro, M. Takahashi, and S. Takahashi, *J. Vac. Sci. Technol. A* **3**, 1502 (1985).  
<sup>13</sup>St. Tosch and H. Neddermeyer, *Phys. Rev. Lett.* **61**, 349 (1988).  
<sup>14</sup>U. K. Kohler, J. E. Demuth, and R. J. Hamers, *Phys. Rev. Lett.* **60**, 2499 (1988).  
<sup>15</sup>G. LeLay, M. Manneville, and R. Kern, *Surf. Sci.* **65**, 261 (1977).  
<sup>16</sup>J. J. Metois and G. LeLay, *Surf. Sci.* **133**, 422 (1983).  
<sup>17</sup>R. M. Feenstra, J. A. Stroscio, and A. P. Fein, *Surf. Sci.* **181**, 295 (1987).

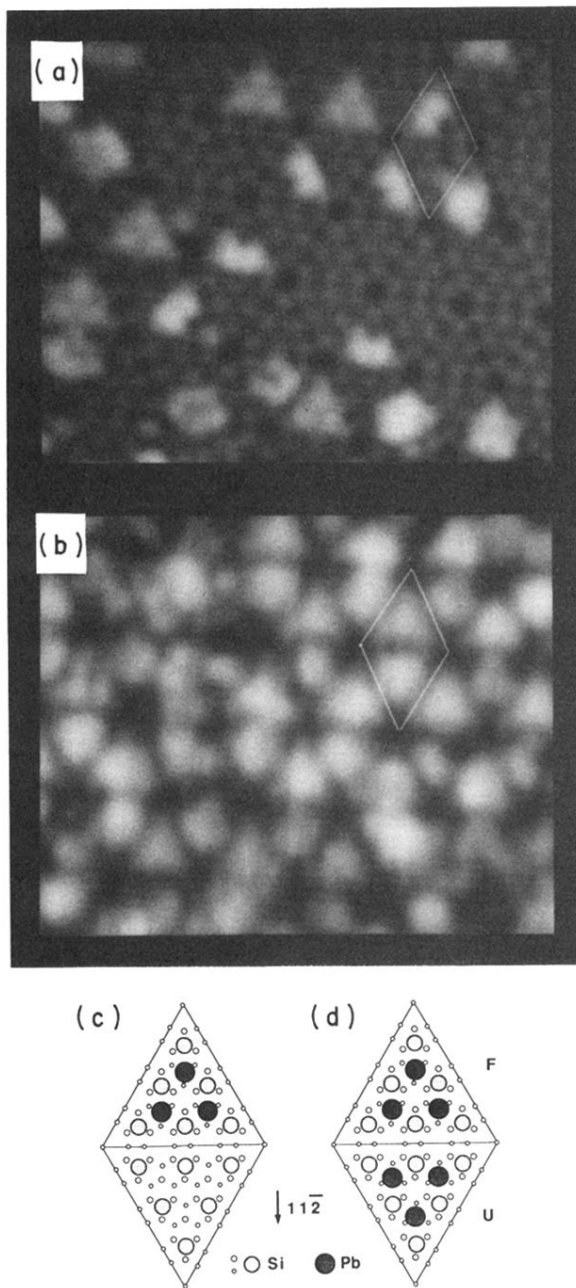


FIG. 1.  $120 \times 140 \text{ \AA}^2$  tunneling images of (a) 0.04-ML Pb, and (b) 0.15-ML Pb deposited onto Si(111)  $7 \times 7$  at RT. Models showing Pb adatom positions for (c) 0.06-ML Pb, and (d) 0.12-ML Pb. The Pb adatoms are above and between the Si adatoms. Small circles represent first and second Si substrate layer, large circles represent Si and Pb adatoms. The faulted and unfaulted halves of the  $7 \times 7$  unit cell are indicated.

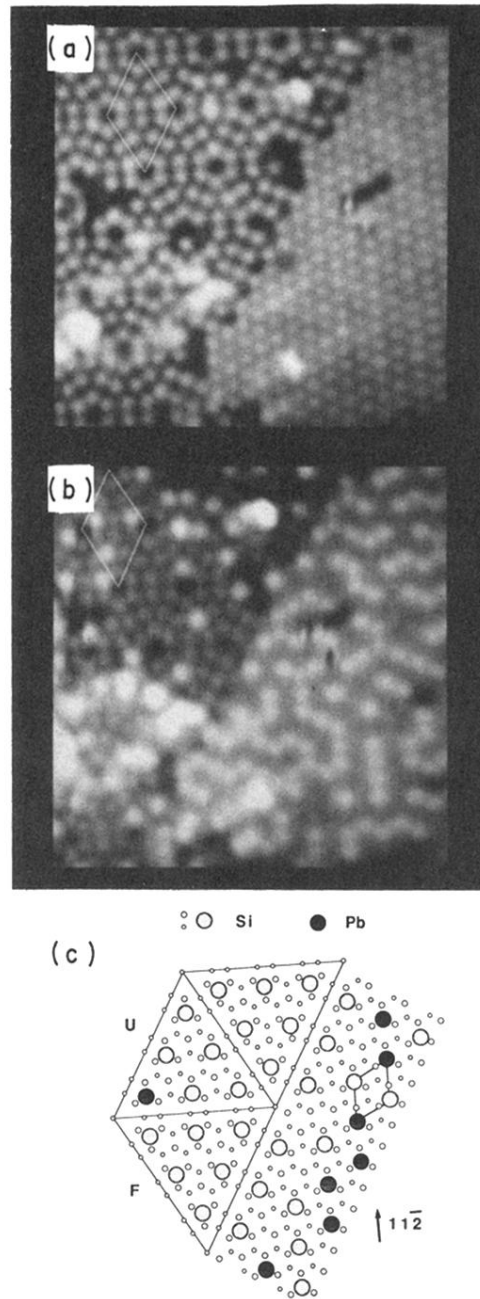


FIG. 3. Two  $150 \times 150 \text{ \AA}^2$  tunneling images of an interface between  $7 \times 7$  and  $\sqrt{3} \times \sqrt{3}$  areas. (a) At 1.65-V bias, Pb and Si atoms are indistinguishable. (b) At 2.3-V bias the Pb atoms appear as bright spots. (c) Model showing the atomic arrangement of the interface at the center of (a) and (b). Small circles represent first and second Si substrate layer, large circles represent Si and Pb adatoms. The faulted and unfaulted halves of the  $7 \times 7$  unit cell are indicated.